Journal of Applied Polymer Science

Kinetic Study of the Dehydrogenation Reaction in Polyacrylonitrile-Based Carbon Fiber Precursors during Thermal Stabilization

Yan Xue, Jie Liu, Jieying Liang
Key Laboratory of Carbon Fiber and Functional Polymers, Ministry of Education, Beijing University of Chemical Technology, Beijing 100029, China

Correspondence to: J. Liu (E-mail: liuj@mail.buct.edu.cn)

ABSTRACT: The kinetics of dehydrogenation reaction and the structural evolution in polyacrylonitrile precursor fibers during thermal stabilization in air have been studied by Fourier transform infrared spectroscopy. The results indicate that, with the progress of dehydrogenation, the absorbance of methylene groups (—CH_2—) gradually decreases, whereas that of methine groups (=CH—) gradually increases. The dehydrogenation reaction in the fibers is basically completed after 20-min stabilization above 255°C. According to the Beer–Lambert law, the values of the absorbance for both —CH_2— groups and the resulting =CH— groups have been calculated and converted into the concentration fractions of —CH_2— groups via the Lorentzian multipeak fitting. According to the principles of chemical kinetics, the dehydrogenation reaction has been determined as a pseudo-second-order reaction with an activation energy of 107.6 kJ mol^{-1}. © 2012 Wiley Periodicals, Inc. J. Appl. Polym. Sci. 000: 000–000, 2012

KEYWORDS: polyacrylonitrile; carbon fiber; thermal stabilization; dehydrogenation; kinetics

Received 16 September 2011; accepted 11 April 2012; published online
DOI: 10.1002/app.37878

INTRODUCTION

Carbon fibers made from the precursor fibers of polyacrylonitrile (PAN) are an important type of structural materials with superior properties including, but not limited to, high tensile strength and Young's modulus, excellent heat resistance, and low density.[1–5] Albeit carbon fibers can also be made from other precursor fibers (e.g., the fibers of petroleum and/or synthetic pitch), PAN fibers are the most commonly adopted precursor for producing carbon fibers with superior tensile strength. Currently, the T1000® carbon fibers produced by Toray Industries (Beijing, China) are among the strongest carbon fibers available commercially; the T1000® carbon fibers possess the tensile strength of ~ 7.1 GPa and a Young's modulus of ~ 290 GPa.[6–10] During the production, PAN undergoes a series of temperature-, atmosphere-, and tension-controlled processes (e.g., stabilization in oxidative environment such as in air and carbonization in inert environment such as in nitrogen).[3,8,11–16] Stabilization is the most complicated and time-consuming steps in the production of carbon fibers[17–19]; in a typical process, PAN precursor fibers are placed in an open air furnace and stabilized for 1–2 h in the temperature range from 180 to 300°C.[2,17,20–23] During the process, a series of gas–solid phase chemical reactions would occur, and these reactions primarily include three types: cyclization, dehydrogenation, and oxidation.[20,24–26] The dehydrogenation reaction results in the formation of carbon–carbon double bond and conjugated structures in the precursor fibers.[17,25,27] This type of reaction together with the cyclization reaction would lead to ladder-like molecular structures, making the oxidized PAN fibers heat resistant and infusible[25,26]; thus, the fibers would maintain the dimensions during the subsequent higher temperature carbonization.[17,27]

It is known that the formation of heat-resistant structures in PAN precursor fibers during thermal stabilization has a vital effect on the ultimate graphite-like structures and mechanical properties of carbon fibers; hence, the in-depth understanding and precise control of thermal stabilization are crucial. To optimize the processing parameters, chemical reactions during thermal stabilization of PAN fibers need to be further investigated, particularly the chemical kinetic mechanisms.

In recent decades, numerous research endeavors on the chemical kinetics of thermal stabilization for PAN fibers have been carried out by thermal analysis techniques, such as the Kissinger method and Ozawa method; nonetheless, most of the

Applied Polymer SCIENCE

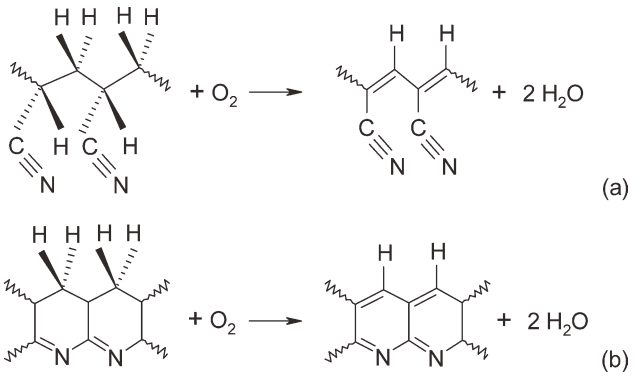

Scheme 1. The dehydrogenation reaction in PAN during thermal stabilization in air: (a) initial PAN, (b) cyclized PAN.

studies only targeted on the cyclization kinetics of various PAN copolymers.[21,26,28–30] For thermal analyses, the differential thermal analysis (DTA) or differential scanning calorimetry (DSC) exotherm of cyclization is usually superposed on that of the dehydrogenation in oxidizing atmosphere; whereas in inert atmosphere, there is only the exotherm of the cyclization.[26,31] Consequently, these two types of reactions cannot be quantitatively investigated simultaneously. Furthermore, the Kissinger method and Ozawa method are designed for the first-order reactions; they might not be applicable to the dehydrogenation and/or oxidation reactions with unknown reaction orders.

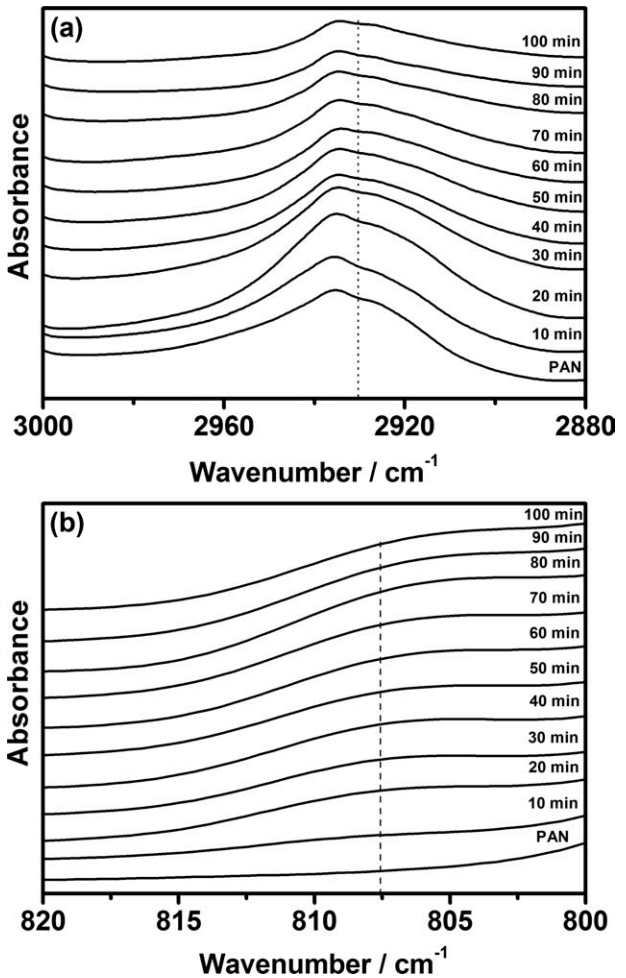

Figure 1. FTIR spectra of PAN precursor fibers stabilized for varied time periods at 225°C: (a) the band of ν_{as}(—CH_2—) and (b) the band of γ(=CH—).

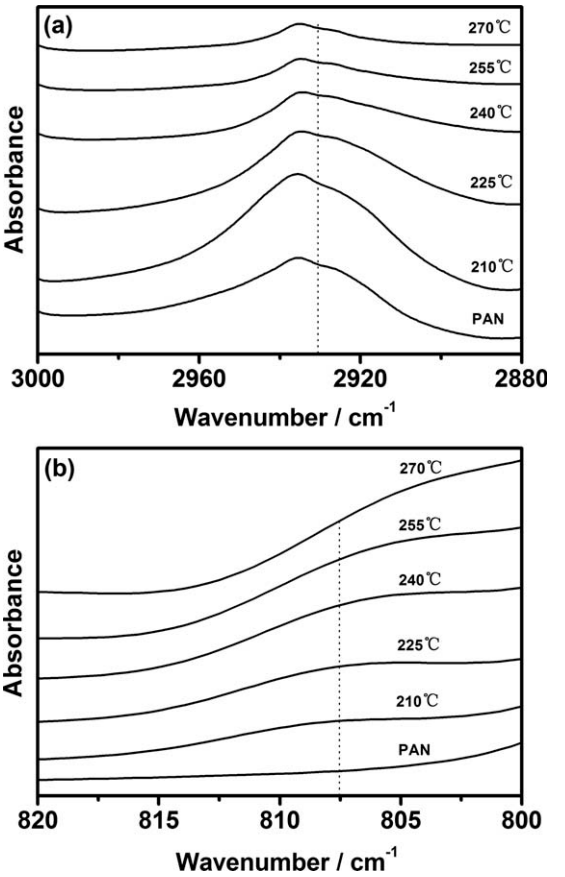

Figure 2. FTIR spectra of PAN precursor fibers stabilized for 30 min at varied temperatures: (a) the band of ν_{as}(—CH_2—) and (b) the band of γ(=CH—).

Fourier transform infrared spectroscopy (FTIR) has often been used to study the structural evolution of PAN during thermal stabilization. The qualitative investigations[32–37] have indicated that IR intensities of the characteristic groups (such as —CH_2—) decrease with the progress of dehydrogenation. Bahrami et al.[35] reported the reaction rate constants of cyclization and dehydrogenation for three different PAN copolymers at 230°C in air; however, they did not confirm the reaction order and activation energy.

In this study, the kinetics of dehydrogenation reaction as well as the structural evolution of an industrial precursor fiber of PAN copolymer during the thermal stabilization in air was quantitatively investigated by FTIR and Lorentzian multipeak fitting. The values of reaction order (n), reaction rate constants (k) at various temperatures, activation energy (E_a), and pre-exponential factor (A) for the dehydrogenation reaction were obtained.

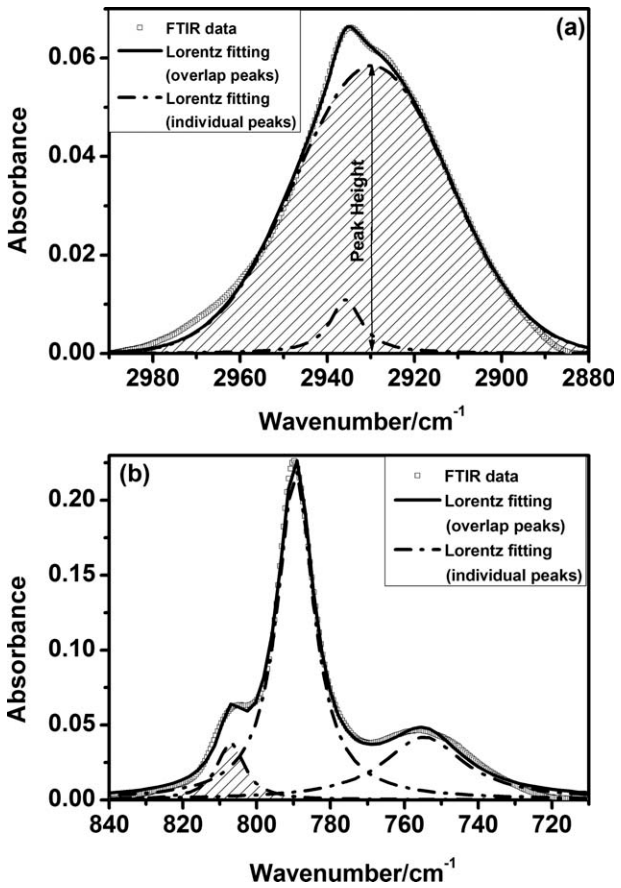

Figure 3. The Lorentzian fitting results for FTIR bands of PAN precursor fibers stabilized at 225°C for 30 min: (a) ν_{as}(—CH_2—) and (b) γ(=CH—).

EXPERIMENTAL

Material

The precursor fibers used in this study were the Special Acrylic Fibers (S.A.F. 3K) provided by the Courtaulds (Nottingham, UK). SAF 3K fibers were in the form of bundle with 3000 individual fibers of a PAN copolymer. Each fiber had the diameter of $\sim$ 11 μm (1.22 dtex), and the copolymer was synthesized from acrylonitrile together with 1.2 wt % of itaconic acid and 6.0 wt % of methyl acrylate.

Thermal Stabilization

The continuous bundle of precursor fibers was first cut into filament tows with the length of 60 cm. These filament tows were then fixed on a stainless steel shelf to keep length and restrain shrinkage during thermal stabilization. Subsequently, the shelf on which filament tows were fixed was placed in an open furnace with constant flow of air. The furnace was set at five different temperatures of 210, 225, 240, 255, and 270°C, respectively; while at each temperature, the samples of oxidized PAN fibers were collected after stabilization for 10–100 min with an interval of 10 min. Finally, 50 samples of oxidized PAN fibers were obtained for FTIR analysis; for comparison, the as-received SAF 3K fibers were also analyzed by FTIR.

FTIR

A Bruker Tensor 27 FTIR spectrometer (Bruker Optics, Germany) equipped with a liquid nitrogen-cooled mercury-cadmium-telluride detector was used to carry out this study. The acquired FTIR spectra had the resolution of 0.5 cm^{-1}, wavenumber precision of 10^{-6} cm^{-1}, and wavenumber range from 400 to 4000 cm^{-1}. For the preparation of FTIR specimens, the fiber samples were first cut into powder; thereafter, $\sim$ 5 mg of each powder sample was ground with 300 mg KBr powder for mixing uniformly. Prior to the preparation, each fiber sample, as well as KBr, was desiccated in a vacuum oven at 60°C for 48 h.

RESULTS AND DISCUSSION

Chemical Reaction and FTIR Analysis

Upon dehydrogenation, carbon–carbon double bonds (—C=C—) and conjugated structures would be generated in PAN precursor fibers. In general, the dehydrogenation reaction includes the processes of oxidation and water removal; these can occur in both initial PAN [Scheme 1(a)] and cyclized PAN [Scheme 1(b)].[17,26]

As illustrated in Scheme 1, there are three carbon atoms in a repeating unit of PAN macromolecule. The first carbon atom bonds to a nitrile group and a hydrogen atom, the second one is the carbon atom in methylene (—CH_2—) group, whereas the third carbon atom is the one in the nitrile group. Upon dehydrogenation, a carbon–carbon double bond (—C=C—) would be generated between the first and second carbon atoms through removal of a hydrogen atom from each of the carbon

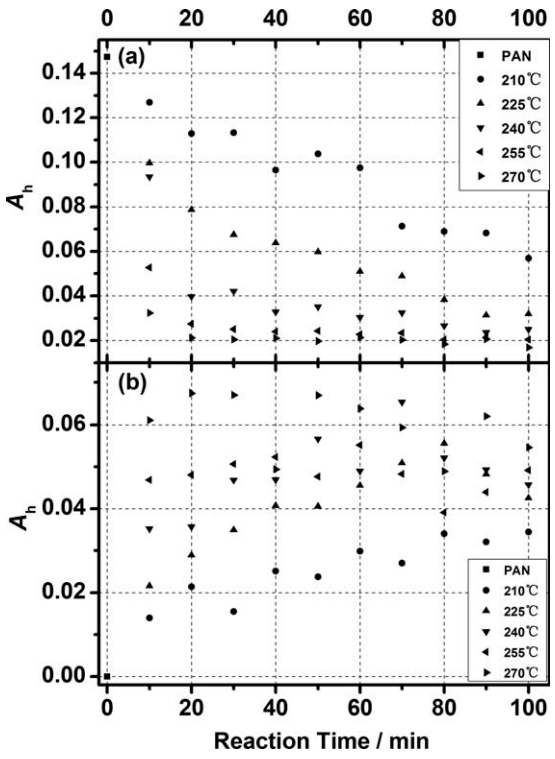

Figure 4. Dependence on the reaction time of the FTIR absorbing peak height (A_h): (a) ν_{as}(—CH_2—) and (b) γ(=CH—).

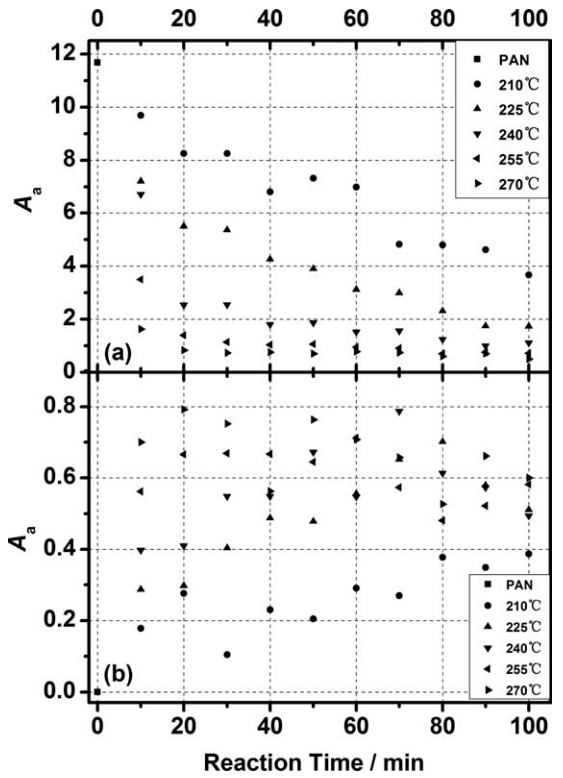

Figure 5. Dependence on the reaction time of the FTIR absorbing peak area (A_a): (a) ν_{as}(—CH_2—) and (b) γ(=CH—).

atom, leading to the conversion of —CH_2— into =CH—. The evidences for the evolution of functional groups can be acquired from the following FTIR analyses.

As shown in Figure 1, the FTIR spectra of PAN precursor fibers stabilized for varied time periods at 225°C illustrate the evolution of functional groups of —CH_2— and =CH— during dehydrogenation. In Figure 1(a), the band centered at $\sim$ 2930 cm^{-1} is assigned to the asymmetric stretching vibration of methylene (viz. ν_{as} in —CH_2—),[32–36] whereas Figure 1(b) shows the band centered at $\sim$ 807 cm^{-1}, which is attributed to the out of plane bending vibration of methine (viz. γ in =CH—).[32,34,37] Figure 1 indicates that, with the progress of stabilization, from the as-received PAN precursor fibers to the fibers treated for 100 min, the band intensity of ν_{as}(—CH_2—) at 2930 cm^{-1} keeps decreasing, whereas that of γ(=CH—) at 807 cm^{-1} keeps increasing. Therefore, as the dehydrogenation proceeds, the amount of —CH_2— continuously decreases due to the conversion of —CH_2— into =CH—.

Figure 2 shows the FTIR spectra of PAN precursor fibers stabilized for 30 min at varied temperatures. Figure 2(a,b) indicates more obviously the decreasing trend of the absorbance for —CH_2— and the increasing trend of the absorbance for =CH— than Figure 1. Upon the examination of Figure 2(a), it is evident that, after as-received PAN fibers undergo the thermal stabilization at temperatures from 210 to 270°C for 30 min, the absorbance of ν_{as}(—CH_2—) band centered at 2930 cm^{-1} becomes lower, indicating that in the case of constant reaction time the reaction degree is enhanced along with the increase of temperature. When the temperature is 255°C or higher, differences of the bands centered at 2930 cm^{-1} are not appreciable; this proves that the dehydrogenation rate considerably decreases after the fibers being stabilized for 30 min at 255°C or higher. On the contrary, in Figure 2(b), the step-like band corresponding to γ(=CH—) centered at 807 cm^{-1} becomes more evident, as the temperature increases. Similar to that in Figure 2(a), the differences of the absorbance curves for the temperature above 255°C are small, indicating that the reaction rate for dehydrogenation reduces after thermal stabilization for 30 min.

Reaction Rate Equation

With the progress of dehydrogenation reaction, —CH_2— groups are gradually converted into =CH— groups. Rendering C(—CH_2—) to represent the amount of methylene and C(=CH—) to represent the amount of methine, the total amount of the repeating units in macromolecular chains remains constant and is represented by C; thus, the fraction of —CH_2—, that is, x(—CH_2—), could be expressed as:

$$x(-CH_2-) = \frac{C(-CH_2-)}{C(-CH_2-) + C(=CH-)} = \frac{C(-CH_2-)}{C} \quad (1)$$

According to the Beer–Lambert law, the concentrations of functional groups have a linear relation with their infrared absorbance. The equations for values of group absorbance are

$$A(-CH_2-) = \varepsilon(-CH_2-) \cdot L \cdot C(-CH_2-) \quad (2)$$

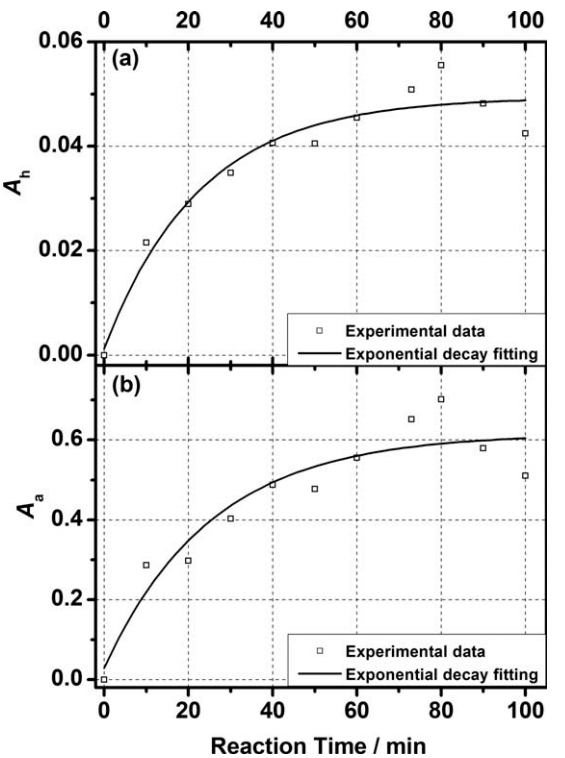

Figure 6. Dependence on the reaction time of the FTIR absorbance of γ(=CH—) for PAN precursor fibers stabilized at 225°C: (a) A_h (IR absorbing peak height) and (b) A_a (IR absorbing peak area).

Table I. Values of r at Varied Temperatures

	Peak height method			Peak area method		
Temperature (°C)	$A(-CH_2-)_0$	$A(=CH-)_\infty$	r	$A(-CH_2-)_0$	$A(=CH-)_\infty$	r
210	0.14728	0.03525	4.18	11.68019	0.55648	20.99
225	0.14728	0.04941	2.98	11.68019	0.61619	18.96
240	0.14728	0.05084	2.90	11.68019	0.63998	18.25
255	0.14728	0.05094	2.89	11.68019	0.67569	17.29
270	0.14728	0.06494	2.27	11.68019	0.73385	15.92

$$A(=CH-) = \varepsilon(=CH-) \cdot L \cdot C(=CH-) \quad (3)$$

where $A(-CH_2-)$ and $A(=CH-)$ are the absorbance values of $-CH_2-$ and $=CH-$, respectively. $\varepsilon(-CH_2-)$ and $\varepsilon(=CH-)$ stand for the absorption coefficient of $-CH_2-$ and $=CH-$, respectively. L is the path length and remains constant, because each sample has the same thickness. The absorbance values can be obtained by the peak height or peak area of FTIR absorption bands for both $-CH_2-$ and $=CH-$.

Hence, $x(-CH_2-)$ can be further written as:

$$x(-CH_2-) = \frac{A(-CH_2-)/[\varepsilon(-CH_2-) \cdot L]}{A(-CH_2-)/[\varepsilon(-CH_2-) \cdot L] + A(=CH-)/[\varepsilon(=CH-) \cdot L]} \quad (4)$$

In this equation, L could be eliminated. Under the definition above,

$$r = \frac{\varepsilon(-CH_2-)}{\varepsilon(=CH-)} \quad (5)$$

is the ratio of the absorption coefficients,[38] eq. (4) could be transformed into

$$x(-CH_2-) = \frac{A(-CH_2-)}{A(-CH_2-) + r \cdot A(=CH-)} \quad (6)$$

Referring to Scheme 1 and the principles of chemical kinetics, the reaction rate equation of the dehydrogenation is

$$-\frac{dx(-CH_2-)}{dt} = k' \cdot x(-CH_2-)^n \cdot x(O_2)^{n'} \quad (7)$$

where t is the reaction time, k' is the reaction rate constant, $x(O_2)$ is the nondimensional concentration of oxygen, n and n' are the reaction orders for $-CH_2-$ and O_2, respectively. As the air is continuously flowed into the furnace, the oxygen concentration can be considered as a constant during the reaction. Therefore, the term of $x(O_2)^{n'}$ combined with k' can be expressed as a constant k. As shown in eq. (8)

$$-\frac{dx(-CH_2-)}{dt} = k \cdot x(-CH_2-)^n \quad (8)$$

the dehydrogenation is thus considered as a pseudo-nth-order reaction.

Multipeak Fitting for FTIR Bands and Evaluation of r

To evaluate the absorbance, the FTIR bands centered at 2930 and 807 cm^{-1} are fitted according to the Lorentzian function. Taking the spectrum of PAN precursor fibers stabilized at 225°C for 30 min, for example, there are two overlap peaks ranging from 2990 to 2880 cm^{-1} in Figure 3(a). These two peaks are fitted according to the Lorentzian function for deconvolution. The absorbing peak around 2930 cm^{-1} is assigned to $\nu_{as}(-CH_2-)$, and the small peak around 2935 cm^{-1} is assigned to the methyl asymmetric stretching vibration (viz. ν_{as} in $-CH_3$). The solid curve is the overall fitting curve. The dash dot curves are individual fitting curves, and the shadow region is the peak area for the absorbing peak around 2930 cm^{-1}. The peak value of individual fitting curve is termed as the peak height (A_h), and the integral area of the shadow is defined as the peak area (A_a).

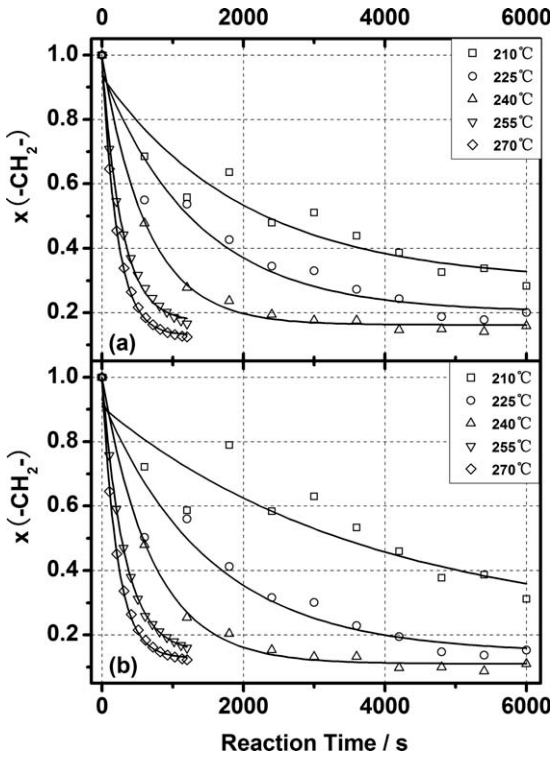

Figure 7. Dependence on the reaction time of the concentration fraction of methylene $x(-CH_2-)$: (a) the peak height method and (b) the peak area method.

Applied Polymer SCIENCE

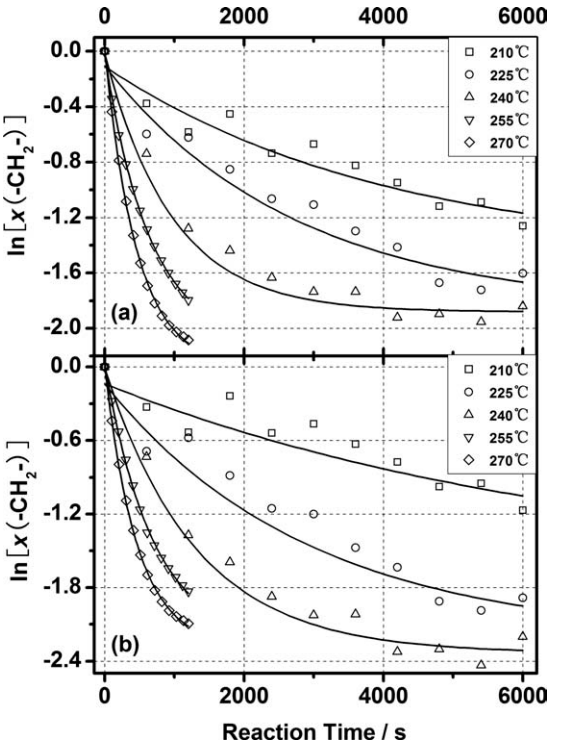

Figure 8. Dependence on the reaction time of $\ln[x(-CH_2-)]$: (a) the peak height method and (b) the peak area method.

In Figure 3(b), there are three peaks ranging from 820 to 730 cm^{-1}, which overlap with each other. For deconvolution of the absorbing peak around 807 cm^{-1}, these overlap peaks are fitted and separated into three individual peaks (dash dot curves). The peak around 807 cm^{-1} (shadow part) is corresponding to $\gamma(=CH-)$. Similarly, A_h and A_a can also be calculated by the fitting function data, and the results are shown in Figures 4 and 5.

Figures 4(a) and 5(a) depict that the FTIR absorbance of methylene gradually decreases during the dehydrogenation reaction. However, the decreasing rate of methylene absorbance is gradually enhanced, and the absorbance profile moves downward from 210 to 270°C, suggesting that the reaction degree has been improved. Between 210 and 240°C, the decreasing rate of absorbance is relatively low as far as 100 min, which is represented by the distinct decay curves; whereas above 255°C the absorbance of $-CH_2-$ rapidly decreases at the beginning of the reaction until 20 min, when a platform period begins till the end. It is demonstrated that the dehydrogenation reaction in PAN precursor fibers is almost completed after 20-min stabilization above 255°C. This may be due to the reason that the tautomerization occurring inside the cyclized structure has replaced the dehydrogenation, cyclization, and oxidation to become the major reaction at certain temperature or time during stabilization[37,39]; hence, the effective reaction time for the dehydrogenation from 255 to 270°C would be 20 min.

Figures 4(b) and 5(b) depict that the FTIR absorbance of methine increases with the progress of dehydrogenation. In addition, from 210 to 270°C, the absorbance profile moves upward, suggesting that the reaction degree is enhanced. Furthermore, between 210 and 240°C, the increasing rate of absorbance is relatively low till 100 min, which appears to be logistic curves. Above 255°C, the absorbance of $=CH-$ rapidly increases at the beginning of the reaction until 20 min, and then a platform occurs for a short time period. Subsequently, the absorbance of $=CH-$ tends to decrease from 50 min to the end. This is probably due to the oxidation that converts $=CH-$ into oxygen-containing groups[39] and eventually makes the methine absorbance decrease.

The ratio of the absorption coefficients (r) can be calculated by the limit method[38] as follows:

$$r = \frac{\varepsilon(-CH_2-)}{\varepsilon(=CH-)} = \frac{A(-CH_2-)_0 / C(-CH_2-)_0}{A(=CH-)_\infty / C(=CH-)_\infty} \quad (9)$$

where $A(-CH_2-)_0$ and $C(-CH_2-)_0$ represent the initial absorbance and concentration of methylene group, respectively, $A(=CH-)_\infty$ and $C(=CH-)_\infty$ mean the methine absorbance and concentration, respectively, at prolonged time after all of methylene groups have reacted. $A(-CH_2-)_0$ is confirmed by the Lorentzian multipeak fitting. Assuming all of methylene groups have been converted into the methine groups as $t \to \infty$, thus $C(-CH_2-)_0 = C(=CH-)_\infty = C$; thus, eq. (9) can be written as:

$$r = \frac{A(-CH_2-)_0}{A(=CH-)_\infty} \quad (10)$$

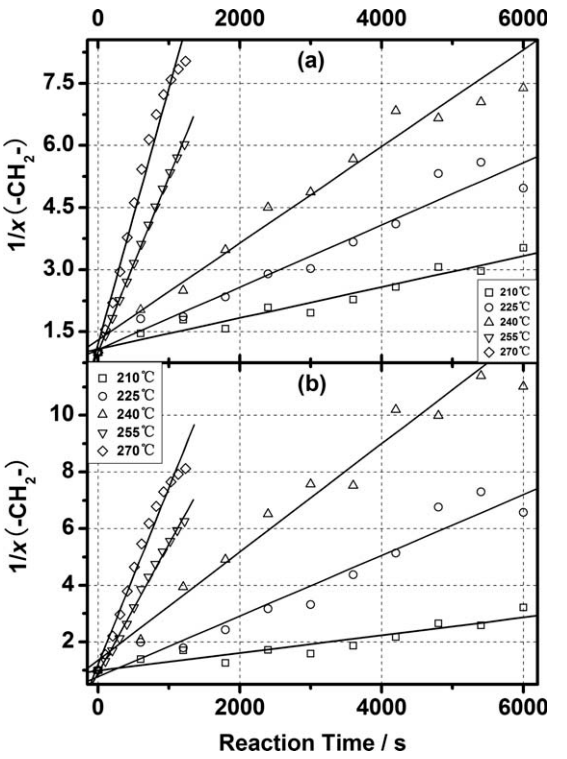

Figure 9. Dependence on the reaction time of $1/x$: (a) the peak height method and (b) the peak area method.

Table II. Values of k at Varied Temperatures (Results Acquired from the Linear Regression)

	Peak height method			Peak area method		
Temperature (°C)	$k \times 10^4$	$S^a \times 10^5$	R^b	$k \times 10^4$	$S \times 10^5$	R
210	3.74	3.03	0.97180	3.13	4.05	0.93220
225	7.47	5.96	0.97254	10.6	8.88	0.97005
240	9.28	6.85	0.98288	16.2	11.5	0.98168
255	42.3	4.46	0.99939	45.7	9.89	0.99743
270	61.8	8.89	0.98820	62.5	8.50	0.98875

[a]Standard error, [b]Correlation coefficient.

The value of $A(=CH-)_\infty$ can be calculated by the nonlinear fitting.

The solid curves in Figure 6 are the fitting curves of absorbance, which are consistent with the first-order exponential decay function; therefore, the relation between A and t is

$$A = A' + a \cdot e^{-t/\tau} \tag{11}$$

where A', a, and τ are constants. Corresponding to the fitting curves in Figure 6, it is obtained that $A' > 0$, $a < 0$ and $\tau > 0$. The value of $A(=CH-)_\infty$ is just the limit of function A as $t \to \infty$, as is shown in the following equation

$$A_\infty = \lim_{t \to +\infty} A = A' + \lim_{t \to +\infty} a \cdot e^{-t/\tau} = A' + 0 = A' \tag{12}$$

Through combination of eq. (10) with the fitting results of $A(=CH-)$, the values of r at varied temperatures are calculated and listed in Table I.

Kinetic Parameters of the Dehydrogenation Reaction

According to the calculated results of $A(-CH_2-)$, $A(=CH-)$, and r, the concentration fraction of methylene, namely, $x(-CH_2-)$ could be obtained by eq. (6), as illustrated in Figure 7.

Figure 7 shows the plots of $x(-CH_2-)$ versus time. The values of scattered points are calculated by the peak height method and peak area method, respectively. In addition, these points are fitted according to the first-order exponential decay function as shown by the curves. Between 210 and 240°C, the profiles of $x(-CH_2-)$ are basically consistent with those of $A(-CH_2-)$ in Figures 4(a) and 5(a), which corresponds to the Beer–Lambert law. Between 255 and 270°C, only from 0 to 20 min, Figure 7 shows the values of $x(-CH_2-)$. In Figures 4 and 5, the dehydrogenation in PAN precursor fibers has only lasted for 20 min between 255 and 270°C. Therefore, the scattered points of absorbance for 255 and 270°C are also fitted according to the first-order exponential decay function as shown in Figure 7; and the fitting function values before 20 min are selected to figure out $x(-CH_2-)$ by eq. (7).

In kinetic equations that coincide with eq. (8), if ln x has a linear relation with t, this reaction is then a first-order reaction; if $1/x^{n-1}$ has a linear relation with t, this reaction is then an nth-order reaction ($n \neq 1$). Based on this principle, the plots of $\ln[x(-CH_2-)]$ versus reaction time are obtained and shown in Figure 8.

In Figure 8, the fitting results are still in accordance with the exponential function, and the degree of decay is enhanced with the increase of temperature; this indicates that ln x does not have a linear relation with t.

Moreover, Figure 9 shows that the profile of $1/x(-CH_2-)$ exhibits a linear relation with t and is fitted according to the linear regression, which has proved that the dehydrogenation in PAN precursor fibers is a pseudo-second-order reaction (viz., $n = 2$) as shown by eq. (8). The reaction rate constants at varied temperatures are represented by the slopes of fitting lines and listed in Table II.

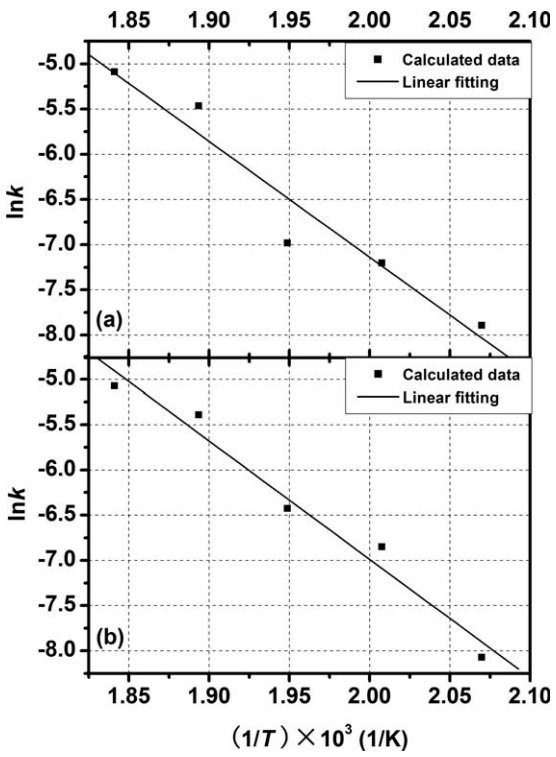

Figure 10. Activation energy analysis: dependence on $1/T$ of ln k, (a) the peak height method and (b) the peak area method.

Table III. Values of E_a and A (Results Acquired from the Linear Regression)

Method	$-E_a/R$	E_a (kJ mol^{-1})	ln A	A
Peak height method	−12,800.3	106.42	18.46	1.04×10^8
Peak area method	−13,083.9	108.78	19.18	2.14×10^8

Referring to the Arrhenius equation,

$$\ln k = \ln A - \frac{E_a}{R}\frac{1}{T} \tag{13}$$

where E_a is the activation energy, and A is the pre-exponential factor. The plots of ln k versus $1/T$ are shown in Figure 10.

The slopes of fitting lines are obtained via $-E_a/R$, and the intercepts are obtained via ln A. According to the above fitting results, the values of E_a and A are acquired (Table III).

As shown in Table III, the method of peak height and peak area give almost the similar values of E_a, namely, 106.42 and 108.78 kJ mol^{-1}, respectively. Hence, the average value of E_a for the dehydrogenation reaction in PAN precursor fibers is 107.6 kJ mol^{-1}.

CONCLUSIONS

The FTIR spectra of PAN precursor fibers stabilized at different temperatures for varied time periods have been studied to understand the evolution of functional groups. The results indicate that the infrared absorbance of methylene group (—CH_2—) (ν_{as} at 2930 cm^{-1}) in the fibers gradually decreases and that of the generated methine group (=CH—) (γ at 807 cm^{-1}) gradually increases during the thermal stabilization. This indicates the process of the dehydrogenation and the formation of carbon–carbon double bond (—C=C—) and/or conjugated structures in macromolecular chains. The results also indicate that, upon stabilization above 255°C for 20 min, the dehydrogenation reaction is close to completion.

Using the Lorentzian multipeak fitting, the height and area of FTIR absorbing peaks are obtained to represent the absorbance values of functional groups. Through combination with the Beer–Lambert law and the principles of chemical kinetics, the dehydrogenation reaction in PAN precursor fibers during thermal stabilization is determined to be a pseudo-second-order reaction, and the kinetic parameters, namely, k, E_a, and A are obtained. The values of E_a calculated by the peak height method and peak area method are similar, and the average value is 107.6 kJ mol^{-1}.

Jie Liu thanks the supports from the National Natural Science Foundation of China (Grant No. 51073011 and 50673011), the National High Technology Research and Development Program of China ("863 Program", Grant No. 2006AA06Z382), and the National Basic Research Program of China ("973 Program", Grant No. 2006CB605304). The authors are grateful to Prof. Hao Fong for the constructive proposals on manuscript revision.

REFERENCES

1. Morgan, P. E. Carbon Fibers and Their Composites; CRC Press: Boca Raton, FL, **2005.**
2. Cui, C.; Yu, L.; Wang, C. *J. Appl. Polym. Sci.* **2010,** *117*, 1596.
3. Yu, M.; Wang, C.; Zhao, Y.; Zhang, M.; Wang, W. *J. Appl. Polym. Sci.* **2010,** *116*, 1207.
4. Tan, L.; Chen, H.; Pan, D.; Pan, N. *J. Appl. Polym. Sci.* **2008,** *110*, 1997.
5. Zeng, X.; Hu, J.; Zhao, J.; Zhang, Y.; Pan, D. *J. Appl. Polym. Sci.* **2007,** *106*, 2267.
6. Liu, J.; Yue, Z. R.; Fong, H. *Small* **2009,** *5*, 536.
7. Zhou, Z. P.; Liu, K. M.; Lai, C. L.; Zhang, L. F.; Li, J. H.; Hou, H. Q.; Reneker, D. H.; Fong, H. *Polymer* **2010,** *51*, 2360.
8. Lai, C. L.; Zhong, G. J.; Yue, Z. R.; Chen, G.; Zhang, L. F.; Vakili, A.; Wang, Y.; Zhu, L.; Liu, J.; Fong, H. *Polymer* **2011,** *52*, 519.
9. Chen, J. C.; Harrison, I. R. *Carbon* **2002,** *40*, 25.
10. Gupta, A.; Harrison, I. R. *Carbon* **1996,** *34*, 1427.
11. Grove, D. A.; Abhiraman, A. S. *Carbon* **1992,** *30*, 451.
12. Liu, J.; Wang, P. H.; Li, R. Y. *J. Appl. Polym. Sci.* **1994,** *52*, 945.
13. Mukundan, T.; Bhanu, V. A.; Wiles, K. B.; Johnson, H.; Bortner, M.; Baird, D. G.; Naskar, A. K.; Ogale, A. A.; Edie, D. D.; McGrath, J. E. *Polymer* **2006,** *47*, 4163.
14. Godshall, D.; Rangarajan, P.; Baird, D. G.; Wilkes, G. L.; Bhanu, V. A.; McGrath, J. E. *Polymer* **2003,** *44*, 4221.
15. Chae, H. G.; Minus, M. L.; Rasheed, A.; Kumar, S. *Polymer* **2007,** *48*, 3781.
16. Bajaj, P.; Sreekumar, T. V.; Sen, K. *Polymer* **2001,** *42*, 1707.
17. Dunham, M. G.; Edie, D. D. *Carbon* **1992,** *30*, 435.
18. Sanchez-Soto, P. J.; Aviles, M. A.; del Rio, J. C.; Gines, J. M.; Pascual, J.; Perez-Rodriguez, J. L. *J. Anal. Appl. Pyrolysis* **2001,** *58–59*, 155.
19. Fitzer, E.; Frohs, W.; Heine, M. *Carbon* **1986,** *24*, 387.
20. Bashir, Z. *Carbon* **1991,** *29*, 1081.
21. Ouyang, Q.; Cheng, L.; Wang, H. J.; Li, K. X. *Polym. Degrad. Stab.* **2008,** *93*, 1415.
22. Jing, M.; Wang, C. C.; Zhu, B.; Wang, Y. X.; Gao, X. P.; Chen, W. N. *J. Appl. Polym. Sci.* **2008,** *108*, 1259.
23. Yu, M.; Wang, C.; Bai, Y.; Wang, Y.; Zhu, B. *J. Appl. Polym. Sci.* **2006,** *102*, 5500.
24. Dalton, S.; Heatley, F.; Budd, P. M. *Polymer* **1999,** *40*, 5531.
25. Rahaman, M. S. A.; Ismail, A. F.; Mustafa, A. *Polym. Degrad. Stab.* **2007,** *92*, 1421.

26. Fitzer, E.; Muller, D. J. *Carbon* **1975,** *13*, 63.
27. Donnet, J. B.; Wang, T. K.; Peng, J. C. M.; Rebouillat, S. Carbon Fiber, 3rd ed.; Marcel Dekker Inc.: New York, **1998.**
28. Devasia, R.; Reghunadhan Nair, C. P.; Sivadasan, P.; Katherine, B. K.; Ninan, K. N. *J. Appl. Polym. Sci.* **2003,** *88*, 915.
29. Ouyang, Q.; Cheng, L.; Wang, H. J.; Li, K. X. *J. Therm. Anal. Calorim.* **2008,** *94*, 85.
30. Belyaev, S. S.; Arkhangelsky, I. V.; Makarenko, I. V. *Thermochim. Acta* **2010,** *507–508*, 9.
31. Beltz, L. A.; Gustafson, R. R. *Carbon* **1996,** *34*, 561.
32. Boccara, A. C.; Fournier, D.; Kumar, A.; Pandey, G. C. *J. Appl. Polym. Sci.* **1997,** *63*, 1785.
33. Varma, S. P.; Lal, B. B.; Srivastava, N. K. *Carbon* **1976,** *14*, 207.
34. Zhang, W. X.; Liu, J.; Wu, G. *Carbon* **2003,** *41*, 2805.
35. Bahrami, S. H.; Bajaj, P.; Sen, K. *J. Appl. Polym. Sci.* **2003,** *88*, 685.
36. Sen, K.; Bajaj, P.; Sreekumar, T. V. *J. Polym. Sci. Part B: Polym. Phys.* **2003,** *41*, 2949.
37. Sivy, G. T.; Gordon, B.; Coleman, M. M. *Carbon* **1983,** *21*, 573.
38. Collins, G. L.; Thomas, N. W.; Williams, G. E. *Carbon* **1988,** *26*, 671.
39. Watt, W.; Johnson, W. *Nature* **1975,** *257*, 210.